

# Functionally Distinct Circuits Are Linked by Heterocellular Electrical Synapses in the Thalamic Reticular Nucleus

 Mitchell J. Vaughn, Zachary Laswick, Huaixing Wang, and  Julie S. Haas

Department of Biological Sciences, Lehigh University, Bethlehem 18015, Pennsylvania

## Abstract

The thalamic reticular nucleus (TRN) inhibits sensory thalamocortical relay neurons and is a key regulator of sensory attention as well as sleep and wake states. Recent developments have identified two distinct genetic subtypes of TRN neurons, calbindin-expressing (CB) and somatostatin-expressing (SOM) neurons. These subtypes differ in localization within the TRN, electrophysiological properties, and importantly, targeting of thalamocortical relay channels. CB neurons send inhibition to and receive excitation from first-order thalamic relay nuclei, while SOM neurons send inhibition to and receive excitation from higher-order thalamic areas. These differences create distinct channels of information flow. It is unknown whether TRN neurons form electrical synapses between SOM and CB neurons and consequently bridge first-order and higher-order thalamic channels. Here, we use GFP reporter mice to label and record from CB-expressing and SOM-expressing TRN neurons. We confirm that GFP expression properly differentiates TRN subtypes based on electrophysiological differences, and we identified electrical synapses between pairs of neurons with and without common GFP expression for both CB and SOM types. That is, electrical synapses link both within and across subtypes of neurons in the TRN, forming either homocellular or heterocellular synapses. Therefore, we conclude that electrical synapses within the TRN provide a substrate for functionally linking thalamocortical first-order and higher-order channels within the TRN.

**Key words:** electrical synapse; gap junction; thalamocortical; thalamus

Received July 31, 2023; revised Nov. 10, 2023; accepted Dec. 18, 2023.

The authors declare no competing financial interests.

Author contributions: M.J.V. and J.S.H. designed research; M.J.V., Z.L., H.W., and J.S.H. performed research; J.S.H. analyzed data; M.J.V. and J.S.H. wrote the paper.

We thank Euan Forrest for data collection efforts and all members of the Haas laboratory for input and discussion. Whitehall Grant in Aid, NIH R01 NS128713.

Correspondence should be addressed to Julie S. Haas at [juliehaas@lehigh.edu](mailto:juliehaas@lehigh.edu).

Copyright © 2024 Vaughn et al. This is an open-access article distributed under the terms of the [Creative Commons Attribution 4.0 International license](https://creativecommons.org/licenses/by/4.0/), which permits unrestricted use, distribution and reproduction in any medium provided that the original work is properly attributed.

## Significance Statement

The thalamic reticular nucleus (TRN) has key roles in sleep, attention, and seizures. Recent work has identified distinct primary and higher-order channels of thalamocortical information flow, but whether and how those channels interact within the TRN is unknown. Intra-TRN communication occurs via a dense network of electrical synapses. Here, we leveraged genetic tools and patch clamping to test whether electrical synapses couple TRN neurons of different subtypes and thereby provide a link between information channels. We found that TRN neurons promiscuously form electrical synapses within and across genetic subtypes, providing a new role for the electrical synapses of the TRN.

## Introduction

Arising sensory signals travel through the thalamus en route to further processing by the cortex. The thalamic reticular nucleus (TRN) is a shell of GABAergic neurons surrounding the dorsal thalamus (Pinault, 2004) that interface the flow of sensory signals by providing the major source of inhibition to thalamic relay neurons and nuclei (Minderhoud, 1971; Jones, 1975; Ohara, 1988; Pinault and Deschenes, 1998). The TRN receives inputs from most thalamic areas (Jones, 1975; Ohara and Lieberman, 1985; Fosse et al., 1986;

Fitzpatrick et al., 1994; Liu and Jones, 1999) as well as deep layers of the cortex (Jones, 1975; Bromberg et al., 1981; Fonnum et al., 1981; Feig and Harting, 1998; Zhang and Jones, 2004; Whilden et al., 2021; Carroll et al., 2022) and a variety of modulatory sources (Anaya-Martinez et al., 2006; Zikopoulos and Barbas, 2012; Aizenberg et al., 2019). Inhibitory signals from the TRN to the thalamus are key regulators of sleep states (Steriade, 2005; Ni et al., 2016; Fernandez et al., 2018; Vantomme et al., 2019) and are responsible for thalamic and cortical spindle generation during sleep (Halassa et al., 2011; Thankachan et al., 2019) as well as cortical slow wave activity during sleep and absence seizures (Inoue et al., 1993; Destexhe, 1998; Steriade, 2005; Lewis et al., 2015; McCafferty et al., 2018). Due to its anatomical and circuit positioning, the TRN has been suggested to focus an attentional spotlight on specific items within the sensory surround (Crick, 1984; McAlonan et al., 2006), and several lines of behavioral evidence support its pivotal role in attention-based tasks (Zikopoulos and Barbas, 2012; Halassa et al., 2014; Wimmer et al., 2015; Sherman, 2016; Nakajima et al., 2019).

Within the TRN, subdivisions by primary sensory modalities have long been established (Pinault, 2004). Early work identified the TRN as a homogeneous population of GABAergic neurons that express parvalbumin (PV; Jones and Hendry, 1989; Seto-Ohshima et al., 1989; Frassoni et al., 1991) with some distinctions between cell types proposed based on cellular anatomy and molecular expression (Bendotti et al., 1990; Mitrofanis, 1992b; Cox et al., 1996; Crabtree, 1996; Lizier et al., 1997; Pinault and Deschenes, 1998; Lam and Sherman, 2007). Recent results leveraging genetic targeting have established a more precise subdivision of TRN neurons, which ties molecular expression to thalamic connectivity. These were first distinguished by PV and somatostatin (SOM) expression (Clemente-Perez et al., 2017). Subsequent work has also distinguished types by calbindin (CB) and SOM expression (Martinez-Garcia et al., 2020) and by a gradient of transcription factor expression (Li et al., 2020). SOM neurons expressing the transcription factor Ecel1 compose the outer shell of the TRN, while PV or CB neurons expressing the transcription factor SPP1 compose the core of the TRN. These subtypes also differ in intrinsic neuronal properties, such as the low-threshold calcium current underlying bursts of action potentials (Clemente-Perez et al., 2017; Li et al., 2020; Martinez-Garcia et al., 2020). Importantly, these distinct neuronal subtypes have also been shown to reciprocally synapse with functionally distinct thalamic targets: SOM neurons reciprocally connect to higher-order thalamic nuclei, areas driven by inputs from cortex, while CB or PV neurons reciprocally connect to the first-order thalamus, areas that are driven by prethalamic afferents (Clemente-Perez et al., 2017; Martinez-Garcia et al., 2020). Cortical input from layers 5 and 6 to the TRN is also organized by shell and core distributions (Whilden et al., 2021; Carroll et al., 2022). Together, the first-order thalamocortical channel consists of primary thalamic nuclei, CB TRN neurons, and cortical input from layer VI, while the higher-order thalamocortical channel comprises higher-order thalamic nuclei, SOM TRN neurons, and cortical input from both layers V and VI. Whether and how these parallel information channels interact within the TRN is unknown.

Synaptic connections between TRN neurons may include GABAergic contacts (Deleuze and Huguenard, 2006; Lam and Sherman, 2007), although these seem to be pruned by the second postnatal week (Hou et al., 2016). The main source of connectivity within the TRN is thought to be its dense and powerful electrical synapses (Landisman et al., 2002; Hou et al., 2016). These synapses have been shown to coordinate TRN rhythms (Fuentealba et al., 2004; Long et al., 2004; Haas and Landisman, 2011), temporally shape the relay of signals through thalamocortical channels (Pham and Haas, 2018), and depress or potentiate as a result of the two distinct TRN activity patterns, bursting, and tonic spikes (Haas et al., 2011; Fricker et al., 2021). Electrical synapses are stronger and more common with closer intersomatic distance (Landisman et al., 2002; Deleuze and Huguenard, 2006; Lee et al., 2014). Understanding of the organization of electrical synapses and networks within the TRN is thus far limited to anatomical work, where dye coupling has shown that network shape appears to vary with position (Lee et al., 2014). Whether electrical synapses couple similar or disparate sets of TRN neurons is unknown. Across the central nervous system, electrical synapses have mostly been shown to couple similar classes or subtypes of neurons (Galarreta and Hestrin, 1999; Gibson et al., 1999; Onn and Grace, 1999; Tamás et al., 2000; Venance et al., 2000; Deans et al., 2001; Schoppa and Westbrook, 2002; Beierlein et al., 2003; Blatow et al., 2003; Chu et al., 2003; Galarreta et al., 2004; Dugué et al., 2009; Curti et al., 2012; Fernandez et al., 2022), but reports of coupling between electrophysiologically distinct classes have been made (Venance et al., 2000; Simon et al., 2005; Zsiros and Maccaferri, 2005; Bloomfield and Volgyi, 2009; Apostolides and Trussell, 2013; Hatch et al., 2017; Kocaturk et al., 2022). In the retina, coupling between cone bipolar cells mixes signals from otherwise parallel channels (Sigulinsky et al., 2020).

To determine whether thalamocortical information channels interact via electrical synapses in the TRN, we used SOM-Cre and CB-Cre mice to identify and electrophysiologically characterize a large cohort of TRN neurons of each genetic subtype *in vitro*. Our results describe a set of intrinsic passive and active differences between genetically labeled SOM and CB neurons. We note that acceleration within a burst, a criterion often used to identify TRN neurons in recordings *in vivo*, is robust for CB neurons but rare for SOM neurons. Our recordings revealed electrical synapses linking both TRN neurons of the same subtype (homocellular synapses) and different subtypes (heterocellular synapses). Heterocellular coupling was confirmed by differences in electrophysiological properties between coupled neurons that matched their genetic labeling. We conclude that heterocellular electrical synapses in the TRN form networks that provide a basis for synaptic interactions between thalamocortical first-order and higher-order channels.

## STAR Methods

### Contact for reagent and resource sharing

Further information and requests for resources and reagents should be directed to and will be fulfilled by the lead contact.

### Experimental model and subject details

All experiments were performed in accordance with the federal IACUC animal welfare guidelines.

**Animals.** We used offspring from SOM-Cre (Jax: 013044) and CB-Cre mice (Jax: 028532) crossed with Ai6 GFP reporter mice (Jax: 007906) of both sexes aged postnatal days (P) 11–28. Mice were anesthetized by inhaled isoflurane (5 ml of isoflurane applied to fabric, within a 1 L chamber) and killed via decapitation.

**Electrophysiology.** Horizontal brain slices 300  $\mu\text{m}$  thick were cut and incubated in sucrose solution (in mM): 72 sucrose, 83 NaCl, 2.5 KCl, 1 NaPO<sub>4</sub>, 3.3 MgSO<sub>4</sub>, 26.2 NaHCO<sub>3</sub>, 22 dextrose, 0.5 CaCl<sub>2</sub>. Slices were incubated at 37°C for 30 min in sucrose following cutting and returned to ACSF at room temperature until recording. The artificial cerebral spinal fluid bath during recording contained the following (in mM): 126 NaCl, 3 KCl, 1.25 NaH<sub>2</sub>PO<sub>4</sub>, 2 MgSO<sub>4</sub>, 26 NaHCO<sub>3</sub>, 10 dextrose, and 2 CaCl<sub>2</sub>, 315–320 mOsm L<sup>-1</sup>, saturated with 95% O<sub>2</sub>/5% CO<sub>2</sub>. The submersion recording chamber was held at 34°C (TC-324B, Warner Instruments). Electrodes were filled with the following (in mM): 135 potassium gluconate, 2 KCl, 4 NaCl, 10 HEPES, 0.2 EGTA, 4 ATP-Mg, 0.3 GTP-Tris, and 10 phosphocreatine-Tris, pH 7.25 (295 mOsm L<sup>-1</sup>). A 1 M KOH was used to adjust pH of the internal solution. The approximate bath flow rate was 2 ml min<sup>-1</sup>, and the recording chamber held ~5 ml solution.

The TRN was visualized under 4 $\times$  magnification, and pairs of adjacent TRN cells from any sensory sector were identified and patched under 40 $\times$  IR-DIC optics (SliceScope, Scientifica). Cell type was initially determined by GFP epifluorescence in the patched neurons. Cells with low fluorescent contrast were avoided. The GFP reporter was excited by a 472 nm diode delivered through the objective (CoolLED pE-300). Voltage signals were amplified and low-pass filtered at 8 kHz (MultiClamp, Axon Instruments, Molecular Devices) and digitized at 20 kHz with custom Matlab routines controlling a National Instruments (USB6221 DAQ board), and data were stored for offline analysis in Matlab (MathWorks, R2018b). Recordings were made in whole-cell current-clamp mode. Negative current was used to maintain cells at -70 mV during recordings. Current injections (500 ms) were used to measure intrinsic properties and coupling. Pipette resistances were 5–9 M $\Omega$  before bridge balance; recordings were discarded if access resistance exceeded 25 M $\Omega$ . Voltages are reported uncorrected for the liquid junction potential.

**Numerical analysis.** Significance tests are two-tailed Mann–Whitney. To measure intrinsic electrophysiological properties, we stimulated each neuron of a pair separately with 500 ms current pulses from -100 to +250 pA in steps of 25 pA.  $R_{in}$  was calculated using the change in membrane voltage divided by the change in applied current, averaged across the first four stimuli (-100, -75, -50, -25 pA). Peak burst rate was the inverse of the fastest interspike interval during a burst, computed for the first trace in which the neuron spiked (rheobase). We identified bursts as the spikes within the first 100 ms after the first spike, or before firing rate fell below 20 Hz, whichever came first. FI gain for tonic spikes was computed as the average firing rate in the last 200 ms of stimulation divided by the amplitude of the applied current, averaged over the set of traces in which the neuron spiked during that time. Acceleration was measured by dividing the first interspike interval by the smallest interspike interval, computed for the rheobase burst and bursts with >2 spikes. Instantaneous frequency was the inverse of each interspike interval. We measured coupling between neurons by delivering a -100 pA, 500 ms current to one neuron and measuring voltage deflections in both neurons. The amplitude of hyperpolarizing current was chosen to minimize activation of voltage-dependent conductances that could distort coupling measurement (Curti and Pereda, 2004; Haas and Landisman, 2011; Li et al., 2023). These currents were repeated 10 times for each neuron of the pair. Coupling coefficient (cc) was calculated as the ratio of voltage changes, of unstimulated neuron to the stimulated neuron, averaged over 10 trials and averaged over both directions of measurement. Coupling conductance was estimated as the inverse of junctional resistance (Fortier, 2010; Haas et al., 2011).

**Data availability.** Datasets collected and analyzed from this study are available upon reasonable request to the corresponding author.

## Results

### SOM and CB neurons are distinguished by differences in intrinsic and bursting properties

SOM and CB (or PV) neurons have distinguishable electrophysiological properties in adult tissue, particularly differences in bursting properties (Clemente-Perez et al., 2017; Li et al., 2020; Martinez-Garcia et al., 2020). All previous electrophysiological investigations of electrical synapses in the TRN using paired recordings have used juvenile tissue (Landisman et al., 2002; Landisman and Connors, 2005; Parker et al., 2009; Haas et al., 2011; Haas and Landisman, 2011; Oh et al., 2014;

Sevetson and Haas, 2015; Wang et al., 2015; Kohmann et al., 2016; Zolnik and Connors, 2016; Sevetson et al., 2017; Fricker et al., 2021) due to the visual occlusion that results from relay neuron myelination in adult tissue. Our goal to widely sample coupling between TRN neuronal subtypes was subject to the same limitation. Juvenile TRN neurons of the age range used here have acquired adult properties (Warren and Jones, 1997; Degen et al., 2004; Cueni et al., 2008; Parker et al., 2009). We ultimately aimed to test for coupling between neurons of different subtypes labeled by GFP in reporter-crossed mice. A possible confound for our coupling measurements is overexpression of GFP due to genetic recombination early in development that might result in persistent GFP reporting (Hu et al., 2013) in crossed mice, which could blur distinctions between cell types. Thus, we first aimed to confirm that our GFP-identified juvenile SOM and CB neurons exhibit distinct sets of intrinsic and spiking properties that have been distinguished in adulthood.

We crossed SOM-Cre (Jax: 013044) or CB-Cre mice (Jax: 028532) with Ai6 GFP reporter mice (Jax: 007906) in order to label specific TRN neuronal subtypes with GFP. We denote neurons that do and do not express GFP in SOM-Cre  $\times$  GFP mice as SOM and non-SOM, respectively, and similarly CB or non-CB for progeny of CB-Cre mice crossed with the Ai6 GFP reporter. In live fluorescence and differential interference contrast (DIC) images of horizontal slices containing the TRN prepared from progeny aged P11-P28, SOM neurons were distributed along the edges of the TRN (Fig. 1A) and CB neurons were densest in the core (Fig. 1C), similar to the previous report (Martinez-Garcia et al., 2020) of virally injected animals.

We recorded from a total of 154 SOM and 107 CB TRN neurons identified by GFP expression, as well as 53 non-GFP-expressing neighboring cells, in current clamp from juvenile brain slices containing the TRN. We maintained neurons at  $-70$  mV in current clamp and applied current steps ranging from  $-100$  to  $+250$  pA in steps of  $25$  pA to each neuron; the sub- and supra-threshold responses (Fig. 1B,D) to current steps allowed us to measure a host of electrophysiological properties and to test for coupling between those pairs. All neurons recorded were targeted for paired recordings and were in close proximity (measured between soma centers:  $16.5 \pm 0.9$   $\mu$ m in SOM mice and  $17.9 \pm 1.1$   $\mu$ m in CB mice). While we did not target specific sectors of the TRN for recording, most recordings of neurons with mismatched expression were made at expression boundaries, where GFP expression was most mosaic (Extended Data Fig. 1-1). Consistent with previous reports from adult tissue, we noted that juvenile SOM neurons appeared to have larger input resistance, and their

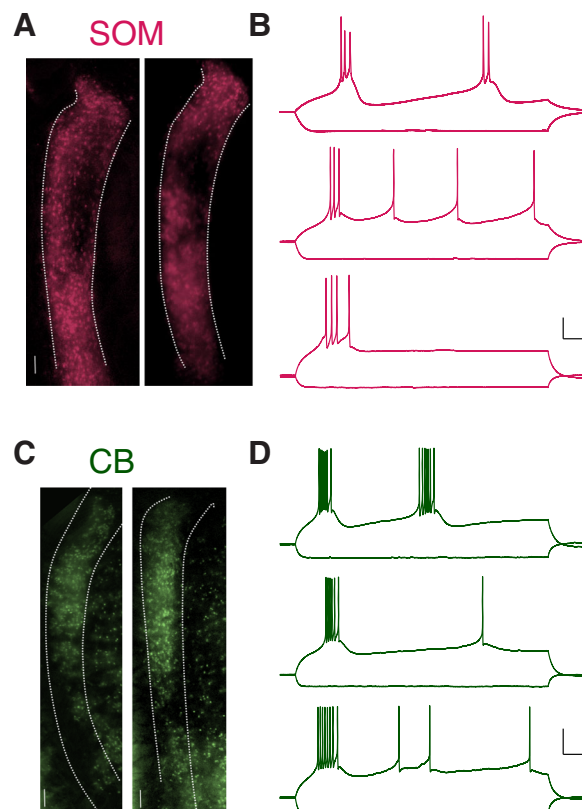


**Figure 1.** Example spatial distributions and spiking responses of SOM and CB neurons in the TRN. **A**, Fluorescence images of a live slice from a SOM  $\times$  Ai6 mouse. SOM-GFP expression, pseudocolored in magenta here, occupies the shell of the TRN. Boundaries were drawn from corresponding IR image. **B**, Example responses of SOM neuron to current steps of  $-100$  pA and rheobase for each cell. From bottom to top,  $V_m = -74.5$ ,  $-74.0$ ,  $-77.0$  mV. Scale bars, 20 mV, 50 ms. **C**, CB-GFP expression in the TRN. **D**, Example responses of CB neuron to current steps of  $-100$  pA and rheobase for each cell. From bottom to top,  $V_m = -74.9$ ,  $-72.7$ ,  $-77.3$  mV. Scale bars, 20 mV, 50 ms. See Extended Data Figure 1-1 for an example of a recording at the boundary between the core and shell of the TRN.

bursts had fewer, slower spikes (Fig. 1B). Spikes within a burst from CB neurons (Fig. 1D) were faster and more numerous. Both SOM and CB neurons emitted tonic spikes following bursts (Fig. 1B,D).

In order to fully characterize differences between GFP-identified SOM and CB neurons, we measured and compared distributions of input resistance, resting membrane potential, threshold, peak spiking rate within a burst, tonic firing gain, maximum tonic spiking rate, acceleration of spikes within a burst, and spikes per burst. In our dataset and similar to a previous report for young adult TRN (Martinez-Garcia et al., 2020), SOM neurons had substantially higher input resistance than CB neurons (Fig. 2A; mean CB  $R_{in}$   $124.6 \pm 4.7$  M $\Omega$ ; mean SOM  $R_{in}$   $222.3 \pm 7.7$  M $\Omega$ ;  $p < 0.01$ ; Mann-Whitney test). Consistent with the report that  $R_{in}$  has stabilized by P11 to  $\sim 200$  M $\Omega$  (Zolnik and Connors, 2016),  $R_{in}$  did not change over the age range of our dataset (Extended Data Fig. 2-1). We found that SOM neurons were slightly depolarized relative to CB neurons ( $V_m$ , mean CB  $-70.0 \pm 0.6$  mV; mean SOM  $-66.6 \pm 0.8$  mV;  $p < 0.01$ ).

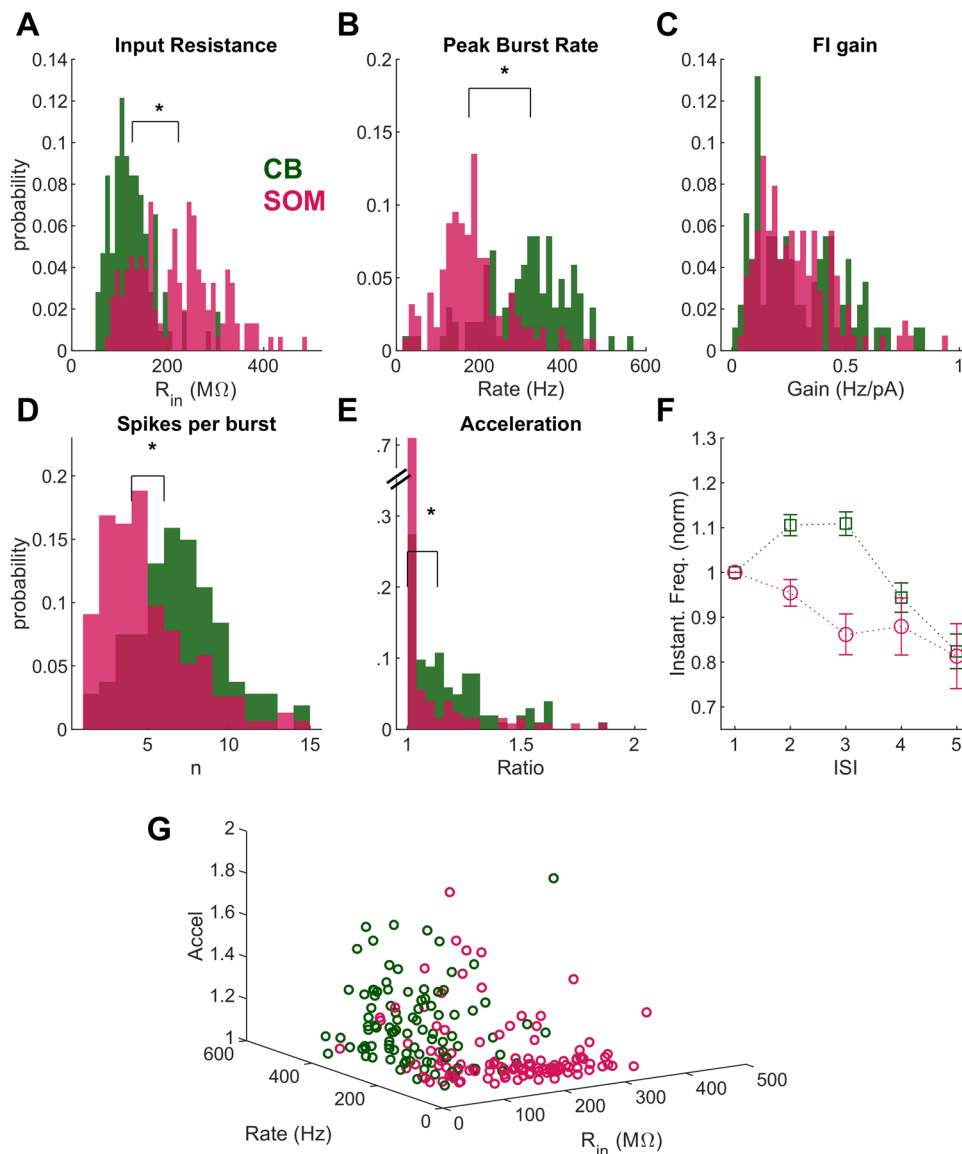


**Figure 2.** Intrinsic and bursting properties distinguish GFP + SOM and CB subtypes in the TRN. **A**,  $R_{in}$  for CB (mean,  $124.6 \pm 4.7$  M $\Omega$ ) and SOM ( $222.3 \pm 7.7$  M $\Omega$ ;  $p < 0.01$ ;  $n = 107$  CB and 154 SOM) neurons. **B**, Peak instantaneous firing rate within bursts for SOM (mean,  $184.4 \pm 7.5$  Hz) and CB ( $312.5 \pm 10.6$  Hz;  $p < 0.01$ ) neurons. **C**, Gain of tonic spiking frequency for SOM and CB neurons (SOM,  $0.37 \pm 0.03$  Hz/pA; CB,  $0.30 \pm 0.02$  Hz/pA;  $p = 0.5$ ). **D**, CB neurons fired more spikes for each burst (SOM,  $4.8 \pm 0.3$  spikes; CB,  $7.0 \pm 0.3$  spikes;  $p < 0.01$ ). **E**, Spiking within a burst accelerated (expressed as the ratio of fastest to first instantaneous rate within the burst) for CB neurons more than for SOM neurons (SOM: median, 1.0, mean,  $1.1 \pm 0.03$ ; CB: median, 1.13, mean,  $1.20 \pm 0.02$ ;  $p < 0.01$ ). **F**, Instantaneous firing for each interspike interval (ISI) within bursts, normalized to the first interval. Data are mean  $\pm$  SEM. **G**, Cell identity as a function of peak burst rate, input resistance, and acceleration ratio. See Extended Data Figure 2-1 for input resistance across age.

Like most thalamic neurons (Steriade and Llinás, 1988; Contreras et al., 1992), TRN neurons fire action potentials in both a calcium burst crowned by a fast barrage of sodium spikes and in trains of regular, or tonic, spikes. We used the burst driven by the rheobase current for each neuron to compare bursts between GFP-expressing types. Several aspects of bursts varied between our SOM and CB TRN neurons. Similar to previous reports, SOM neurons fired fewer spikes within each burst than CB neurons (Fig. 2D; SOM,  $4.8 \pm 0.3$  spikes; CB,  $7.0 \pm 0.3$  spikes;  $p < 0.01$ ). Nineteen SOM neurons and five CB neurons fired only one spike per burst. Within bursts, peak frequency (Fig. 2B) for SOM neurons ( $184.4 \pm 7.5$  Hz) was substantially slower than that for CB neurons ( $312.5 \pm 10.6$  Hz;  $p < 0.01$ ). Spike threshold was lower for SOM neurons (threshold: mean CB,  $-40.1 \pm 0.6$  mV; mean SOM,  $-45.2 \pm 1.1$  mV;  $p = 0.01$ ). Gain of tonic spiking did not differ between CB and SOM neurons (Fig. 2C; mean for SOM,  $0.37 \pm 0.03$  Hz/pA; CB,  $0.30 \pm 0.02$  Hz/pA;  $p = 0.5$ ).

Many reports identify TRN neurons as accelerating within a burst; this is a criterion that is often used to identify TRN neurons within *in vivo* recordings. We measured instantaneous frequency within a burst and quantified acceleration as the ratio of the fastest frequency to the frequency of the first interspike interval within the burst for bursts with  $>2$  spikes (Fig. 2D). In SOM neurons, this ratio was most frequently 1 (median, 1.0; mean,  $1.1 \pm 0.03$ ;  $n = 126$  neurons), indicating a lack of acceleration within bursts. In CB neurons, the ratio was significantly larger (median, 1.13; mean,  $1.20 \pm 0.02$ ;  $p < 0.01$ ;  $n = 102$  neurons for comparison with SOM), reflecting the acceleration commonly observed. Normalized instantaneous frequencies within bursts are shown in Figure 2E, which confirms that the pattern of accelerating spikes within a burst distinguishes CB neurons from SOM neurons in the TRN. Together, our results show that spiking during bursts but not tonic spikes are a distinguishing feature for TRN neurons.

Collectively, these results confirm previous reports that TRN neurons take on mature intrinsic and spiking characteristics by the end of the second postnatal week. Further, they establish that juvenile TRN neurons have already differentiated into the identified SOM and CB subtypes observed in adults and that we can successfully distinguish between those neurons via a combination of GFP labeling and electrophysiological properties (Fig. 2G).

### SOM and CB neurons in the TRN are coupled by both homocellular and heterocellular electrical synapses

Having established that neurons in our juvenile tissue from crossed reporter mice are distinguishable by the same intrinsic and spiking properties that distinguish those neuronal subtypes in adult tissue, we set out to test whether the populations of neuronal subtypes defined by those properties form homocellular and heterocellular electrical synapses. Since it has been previously established that SOM and CB subtypes each interact with distinct thalamocortical information channels, identification of electrical synapses between subtypes will also determine possible avenues for cross talk between those channels within the TRN.

We tested for the presence of homocellular or heterocellular electrical synapses between TRN neurons by patching adjacent pairs that were either SOM/SOM ( $n = 60$  pairs), SOM/non-SOM ( $n = 34$  pairs), CB/CB ( $n = 44$  pairs), or CB/non-CB ( $n = 19$  pairs), as defined by GFP expression. These pairs were composed of the same neurons used to evaluate electrophysiological properties. We tested each pair for the presence of an electrical synapse by applying a 100 pA hyperpolarizing current to one neuron and measuring a hyperpolarizing deflection in the coupled neighbor (Fig. 3A, middle traces). This test was repeated in both directions of current flow across the synapse. Examples of coupling measurements are shown in Figure 3 for SOM/SOM pairs (Fig. 3A), SOM/non-SOM pairs (Fig. 3B), CB/CB pairs (Fig. 3C), and CB/non-CB pairs (Fig. 3D). We identified electrical synapses between all combinations of paired subtypes patched.

For coupled pairs, we calculated coupling coefficient (cc) as the voltage deflection of the unstimulated neuron divided by the voltage deflection in the neuron that received current steps. We considered coupling to exist for  $cc > 0.01$ , based on detectable voltage signals (Extended Data Fig. 4-1). We tested for coupling between a total of 157 pairs that included at least one GFP + neuron. Of our 157 total pairs tested, we found coupling between 30 homocellular SOM/SOM pairs (mean  $cc = 0.06 \pm 0.008$ ; mean  $G_C = 0.30 \pm 0.11$  nS) out of 60 tested pairs and nine homocellular CB/CB pairs (mean  $cc = 0.05 \pm 0.014$ ; mean  $G_C = 0.39 \pm 0.14$  nS) out of 44 tested pairs (Fig. 4A). We found coupling between 23 heterocellular SOM/non-SOM pairs (mean  $cc = 0.06 \pm 0.016$ ; mean  $G_C = 0.25 \pm 0.15$  nS) out of 34 tested pairs, and eight heterocellular CB/non-CB pairs (mean  $cc = 0.05 \pm 0.021$ ; mean  $G_C = 0.32 \pm 0.14$  nS) out of 19 tested pairs (Fig. 4B). These counts reflect a coupling frequency of 50% for SOM pairs and 21% for CB pairs. There were no significant differences between coupling coefficients or conductances between any cell or synapse types, and the frequency of coupling for CB/non-CB and SOM/non-SOM was not significantly different ( $p = 0.09$ ; Fisher's test).

Our data lead us to conclude that unlike interneurons of cortex that preferably form homocellular electrical synapses (Gibson et al., 1999; Beierlein et al., 2003; Blatow et al., 2003; Chu et al., 2003; Galarreta et al., 2004), TRN neurons frequently form both homocellular and heterocellular electrical synapses between neurons of both similar and different types. We suggest that these synapses provide an avenue for interactions between first-order and higher-order thalamocortical relay channels (Fig. 4C).

## Discussion

Cortical attention to the sensory environment is regulated and focused by inhibition from the TRN, an area that also provides one possible key locus for mixing of cortex-bound sensory information. Here, we demonstrate that TRN neurons develop into mature and distinguishable SOM and CB subtypes in juvenile animals, prior to myelination of thalamocortical

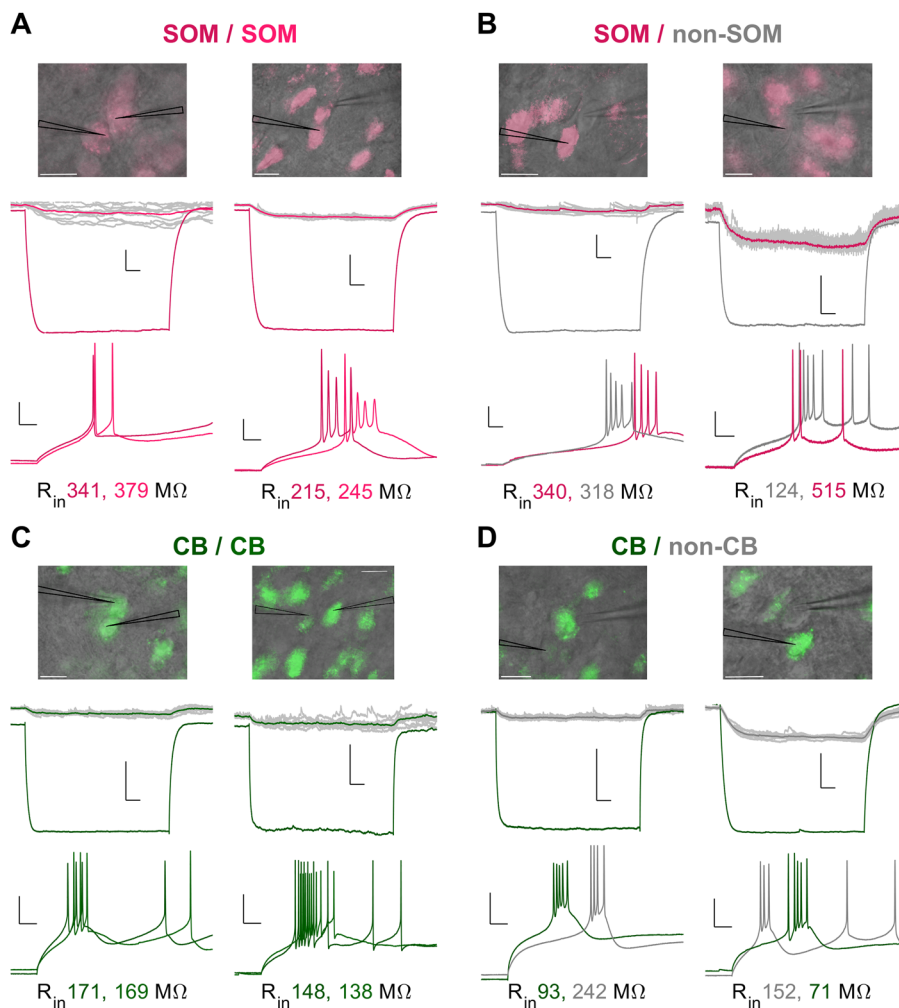


**Figure 3.** Homocellular and heterocellular coupling between pairs of TRN neurons. **A**, Example of coupling between two pairs of SOM neurons. Top, Overlay of fluorescence and DIC images taken during live recordings. Scale bar, 20  $\mu$ m. Middle, Simultaneous voltage responses of both neurons to  $-100$  pA current steps delivered to one neuron of each pair. Scale bars, 5 mV, 50 ms. Bottom, Spiking responses of each neuron to separate injections of rheobase current. Scale bars, 20 ms, 20 mV. **B**, As for **A**, but for pairs of SOM and non-SOM neurons; scale bars in top right are 2.5 mV, 50 ms. **C**, As for **A**, but for pairs of CB neurons. **D**, As for **A**, but for pairs of CB and non-CB neurons.

fibers. Further, we show that SOM and CB neurons form both homocellular and heterocellular electrical synapses. Because SOM neurons have reciprocal connections with higher-order thalamus while CB/PV neurons have distinct reciprocal connections to first-order thalamus (Clemente-Perez et al., 2017; Martinez-Garcia et al., 2020; Hoseini et al., 2021), and given that the two cell types receive inputs from distinct deep layers of cortex (Whilden et al., 2021; Carroll et al., 2022), our results imply that heterocellular coupling links the otherwise distinct first-order and higher-order thalamocortical channels. Conversely, homocellular coupling processes information sent within a thalamocortical relay channel.

We hypothesize that the functions of homocellular and heterocellular synapses share a function of modulating the inhibition delivered to the thalamus, but the impacts of that modulation vary for each synapse type. Coupled TRN neurons of similar subtype could be expected to have similar (but not identical) inputs and outputs, causing homocellular synapses to enhance TRN responses and sensitivity to shared inputs within a sensory modality, resulting in increased and/or better-coordinated thalamic inhibition as a result. Heterocellular coupling provides a substrate for higher-order processes to influence first-order thalamocortical sensory response and relay, dampening it through shared depolarization within the TRN that results in more inhibition to first-order thalamus. Conversely, heterocellular coupling could enhance thalamocortical sensory throughput via shunting across TRN electrical synapses that results in reduced inhibition in the thalamus. Electrical synapses generally facilitate synchronous firing between coupled neurons when they are simultaneously and persistently depolarized (Galarreta and Hestrin, 1999; Gibson et al., 1999; Landisman et al., 2002) and are thus proposed to support rhythms of coupled networks; the variety of coupling shown here could support trans-TRN synchrony initiated by one neuronal subtype.

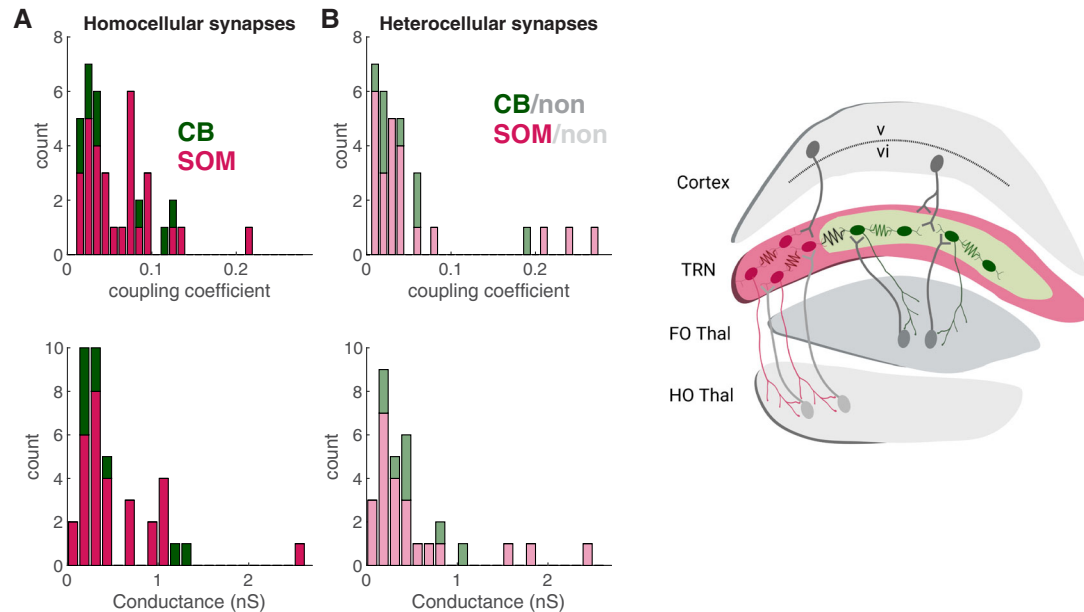


**Figure 4.** Distribution of coupling within and without SOM and CB cell types. **A**, Stacked distribution of homocellular electrical synapses in the TRN; coupling was found between 9 out of 44 pairs of CB neurons tested and 30 out of 60 pairs of SOM neurons tested. cc, coupling coefficient. **B**, Stacked distribution of heterocellular electrical coupling between TRN neurons: synapses were identified between 8 out of 19 pairs of CB and non-CB neurons and 23 out of 34 pairs of SOM and non-SOM neurons tested. **C**, Schematic of distinct thalamocortical pathways linked by electrical synapses of the TRN. FO, first order; HO, higher order. See Extended Data Figure 4-1 for signal-to-noise of coupling measurements.

For transient signals representing sensory inputs to the thalamus, electrical synapses have myriad and more complex effects (Connors, 2017; Alcami, 2018; Vaughn and Haas, 2022). Our previous modeling suggests that TRN electrical synapses aid input discrimination by modulating spike timing in relay neurons (Pham and Haas, 2018), and this effect could be implemented by homocellular synapses to discriminate between similar inputs of the same sensory modality. We noted that coupling was more prevalent between and from SOM neurons, implying that information mixing through electrical synapses is more influential in higher-order thalamocortical systems compared with primary sensory relay.

The heterotypic electrical synapses in our data had mean ccs near 0.05. The strength of synapses we show herein is within the range we previously showed through computational models to alter thalamocortical relay (Pham and Haas, 2018) and coordination of TRN spiking (Mendoza and Haas, 2022). Moreover, *in vitro* experimental work has shown that even the weakest of electrical synapses (cc between 0.01 and 0.05) increase synchrony of subthreshold rhythms (Long et al., 2004). While weaker than other reports for juvenile TRN, homocellular and heterocellular electrical synapses measured here are not unusually weak compared with previous reports of electrical coupling in the inferior olive (Devor and Yarom, 2002) and fast spiking cortical neurons (Deans et al., 2001). In the context of a barrage of synaptic input *in vivo*, we would expect the somatic voltage changes induced by electrical synapses to be reduced, due to the lower input resistance. However, electrical synapses become increasingly relevant during barrages of synaptic inputs because electrical synapses transmit voltage difference, which is how electrical synapses act to improve signal-to-noise ratios and detect coincident inputs to paired neurons (DeVries et al., 2002; Dunn et al., 2006; Medvedev, 2009). Further, many TRN electrical synapses are likely located on dendrites, as they couple TRN neurons with spatially separated somas (Landisman et al., 2002; Lee et al., 2014); thus the voltage changes and coupling measured between somas are smaller than the effective ones locally at dendrites, where the electrical synapses are computationally relevant. Because TRN dendrites are endowed with active T-type calcium channels (Crandall et al., 2010), the local effect of electrical synapses on voltage at dendritic contacts are expected to be particularly important in the TRN. For heterotypic electrical synapses, each side of a coupled dendrite may receive distinct inputs or activation from the different types of thalamocortical channels. Because electrical synapses are driven by voltage differences, heterotypic synapses may be especially impactful in this configuration.

One consideration for hypothesizing about the function of homotypic and heterotypic electrical synapses in the TRN is that electrical synapses are plastic. In the TRN, repeated bursting drives depression of electrical synapses (Haas et al., 2011) and tonic spiking drives long-term potentiation (Fricker et al., 2021). Activation of different mGluRs can also cause either potentiation or depression (Landisman and Connors, 2005; Wang et al., 2015). We speculate that plasticity might be implemented distinctly between hetero- and homosynaptic electrical connections. It is possible that the TRN might maintain heterotypic synapse strength during certain brain states where connection and coordination between first-order and higher-order TRN is desirable, for example, during coordinated sleep rhythms, but be decoupled during wake states. How



homotypic and heterotypic coupling changes in vivo with different wake and sleep states is an exciting question to be investigated in the future.

Acceleration of spikes within bursts has been noted for TRN neurons since early days (Domich et al., 1986; Marlinski and Beloozerova, 2014), and it has been frequently used as an identifier of the TRN for in vivo recordings. Our data clearly demonstrate that only CB neurons in the core of the TRN accelerate, while SOM neurons at the edges of the TRN rarely accelerate during bursts. Thus, it is possible that SOM cells have previously been misidentified as thalamic relay cells in vivo, and results might be re-examined in that context. Certainly, alternative methods such as spike width are necessary to distinguish SOM TRN edge cells from thalamic cells in vivo.

### Limitations of this study

The use of Cre-dependent reporter mice to label genetic subtypes has limitations. Transient expression of Cre during development can cause false expression of the fluorescence in neurons that are negative for the genetic subtype (Hu et al., 2013). This problem has been observed in adult TRN with SOM-Cre mice crossed with a tdTomato reporter mice (Martinez-Garcia et al., 2020). Our results provide evidence that this issue is avoided in juvenile tissue, as GFP expression in juvenile SOM-Cre and CB-Cre TRN was comparable with expression patterns reported in adults utilizing viral injections or in situ hybridization (Fig. 1; Martinez-Garcia et al., 2020; Hoseini et al., 2021). We did observe overexpression of GFP in SOM-Cre mice by adulthood, or after P30 (data not shown), suggesting that Cre recombination from transient SOM expression may not happen early in development, but sometime between eye opening and early adulthood. While we cannot fully rule out overexpression of GFP in our reporter mice, the electrophysiological differences between CB and SOM neurons remained (Fig. 1) and were preserved in heterocellular pairs (Fig. 3), and heterocellular coupling was not a disproportionately rare event (Fig. 4). However, differences in Cre expression could underlie the observed differences in heterotypic synapse incidence between SOM and CB lines. Experiments using a doubly labeled mouse, or post hoc immunostaining of recorded heterocellular pairs, could further enhance the results shown here; we did not perform immunohistochemistry on our tissue. Underexpression of the reporter could also impact labeling of cell types in Cre animals.

Our reports of intrinsic differences are limited to the population of GFP + neurons in our data, and misexpression or lack of GFP could cause homocellular electrical synapses to appear as heterocellular electrical synapses. Further, the overlap and spread of intrinsic properties make classification or identification of any single neuron by its individual properties uncertain. It is possible, though unlikely, that all of the synapses we have identified as heterotypic are misidentified. Therefore, it is possible for future work to refute the claim that TRN cells form both heterocellular and homocellular electrical synapses. However, we find that unlikely given the current dataset; the most supported interpretation is that TRN neurons promiscuously form electrical synapses both within and across subtypes.

The heterocellular coupling observed here occurs at the borders of SOM and CB divisions, which is another distinguishing factor of this cohort of data. Due to the nature of paired recordings, all identified somas were in close proximity to each other; our work implies but cannot fully address the possibility of coupling across larger anatomical distances or sensory sectors of the TRN. Establishing complete maps of electrical synapses across TRN functional groups remains an outstanding goal. The method used here is limited to testing one possible electrical synapse between any two neurons. It is unknown how many electrical synapses, heterocellular or homocellular, a single TRN neuron forms with its neighbors. We also note some differences in incidence and strength from previous reports of coupling in the TRN of rat, which range over mean coupling coefficients between 0.03 and 0.11 and incidence between 31 and 71% (Landisman et al., 2002; Long et al., 2004). These could be attributed to possible differences in species and in experimenter experience and bias in selecting pairs to record. Further, our determination of neuronal subtype is limited by our ability to visualize GFP during live recordings.

Our results are limited to the subtypes of neurons used here: SOM and CB neurons. We did not use PV-Cre mice, as GFP-neurons were absent from previous descriptions of crossed mice (Hou et al., 2016; Thankachan et al., 2019). Two reports suggest PV neurons are a unique subset of the TRN (Clemente-Perez et al., 2017; Hoseini et al., 2021), in a departure from the previous consensus that the TRN is nearly entirely composed of PV-expressing neurons (Seto-Ohshima et al., 1989; Frassoni et al., 1991; Mitrofanis, 1992a; Hou et al., 2016; Thankachan et al., 2019; Li et al., 2020; Martinez-Garcia et al., 2020). The results presented here do not provide any insight to this discrepancy.

Our descriptions of intrinsic differences in  $R_{in}$  are consistent with a previous report of SOM and CB neurons (Martinez-Garcia et al., 2020), but we note that those values differ substantially from reports that distinguish the TRN as comprising overlapping sets of SOM and PV neurons (Clemente-Perez et al., 2017) and for transcriptional differences (Li et al., 2020). Our results are consistent with previous reports of spiking differences between sets of SOM and CB or SOM and PV neurons. Both PV and CB neurons have been described as composing the core of the TRN and reciprocally connecting to primary thalamic nuclei; we thus expect that our CB results herein would also apply to PV neurons.

## References

- Aizenberg M, Martinez SR, Pham T, Rao W, Haas J, Geffen MN (2019) A novel mechanism for amplification of sensory responses by the amygdala-TRN projections. *bioRxiv*:623868.
- Alcami P (2018) Electrical synapses enhance and accelerate interneuron recruitment in response to coincident and sequential excitation. *Front Cell Neurosci* 12:156.
- Anaya-Martinez V, Martinez-Marcos A, Martinez-Fong D, Aceves J, Erij D (2006) Substantia nigra compacta neurons that innervate the reticular thalamic nucleus in the rat also project to striatum or globus pallidus: implications for abnormal motor behavior. *Neuroscience* 143:477–486.
- Apostolides PF, Trussell LO (2013) Regulation of interneuron excitability by gap junction coupling with principal cells. *Nat Neurosci* 16:1764–1772.
- Beierlein M, Gibson JR, Connors BW (2003) Two dynamically distinct inhibitory networks in layer 4 of the neocortex. *J Neurophysiol* 90:2987–3000.
- Bendotti C, Hohmann C, Forloni G, Reeves R, Coyle JT, Oster-Granite ML (1990) Developmental expression of somatostatin in mouse brain. II. In situ hybridization. *Dev Brain Res* 53:26–39.
- Blatow M, Rozov A, Katona I, Hormuzdi SG, Meyer AH, Whittington MA, Caputi A, Monyer H (2003) A novel network of multipolar bursting interneurons generates theta frequency oscillations in neocortex. *Neuron* 38:805–817.
- Bloomfield SA, Volgyi B (2009) The diverse functional roles and regulation of neuronal gap junctions in the retina. *Nat Rev Neurosci* 10:495–506.
- Bromberg MB, Penne JB Jr, Stephenson BS, Young AB (1981) Evidence for glutamate as the neurotransmitter of corticothalamic and corticorubral pathways. *Brain Res* 215:369–74.
- Carroll BJ, Sampathkumar V, Kasthuri N, Sherman SM (2022) Layer 5 of cortex innervates the thalamic reticular nucleus in mice. *Proc Natl Acad Sci U S A* 119:e2205209119.
- Chu Z, Galarreta M, Hestrin S (2003) Synaptic interactions of late-spiking neocortical neurons in layer 1. *J Neurosci* 23:96–102.
- Clemente-Perez A, Makinson SR, Higashikubo B, Brovarney S, Cho FS, Urry A, Holden SS, Wimer M, Dávid C, Fenno LE (2017) Distinct thalamic reticular cell types differentially modulate normal and pathological cortical rhythms. *Cell Rep* 19:2130–2142.
- Connors BW (2017) Synchrony and so much more: diverse roles for electrical synapses in neural circuits. *Dev Neurobiol* 77:610–624.
- Contreras D, Curro Dossi R, Steriade M (1992) Bursting and tonic discharges in two classes of reticular thalamic neurons. *J Neurophysiol* 68:973–977.
- Cox CL, Huguenard JR, Prince DA (1996) Heterogeneous axonal arborizations of rat thalamic reticular neurons in the ventrobasal nucleus. *J Comp Neurol* 366:416–430.
- Crabtree JW (1996) Organization in the somatosensory sector of the cat's thalamic reticular nucleus. *J Comp Neurol* 366:207–222.
- Crandall SR, Govindaiah G, Cox CL (2010) Low-threshold Ca<sup>2+</sup> current amplifies distal dendritic signaling in thalamic reticular neurons. *J Neurosci* 30:15419–15429.
- Crick F (1984) Function of the thalamic reticular complex: the searchlight hypothesis. *Proc Natl Acad Sci U S A* 81:4586–4590.
- Cueni L, Canepari M, Luján R, Emmenegger Y, Watanabe M, Bond CT, Franken P, Adelman JP, Lüthi A (2008) T-type Ca<sup>2+</sup> channels, SK2 channels and SERCAs gate sleep-related oscillations in thalamic dendrites. *Nat Neurosci* 11:683–692.
- Curti S, Pereda AE (2004) Voltage-dependent enhancement of electrical coupling by a subthreshold sodium current. *J Neurosci* 24:3999–4010.
- Curti S, Hoge G, Nagy JI, Pereda AE (2012) Synergy between electrical coupling and membrane properties promotes strong synchronization of neurons of the mesencephalic trigeminal nucleus. *J Neurosci* 32:4341–4359.
- Deans MR, Gibson JR, Sellitto C, Connors BW, Paul DL (2001) Synchronous activity of inhibitory networks in neocortex requires electrical synapses containing connexin36. *Neuron* 31:477–485.
- Degen J, Meier C, Van Der Giessen RS, Söhl G, Petrasch-Parwez E, Urschel S, Dermietzel R, Schilling K, De Zeeuw CI, Willecke K (2004) Expression pattern of lacZ reporter gene representing connexin36 in transgenic mice. *J Comp Neurol* 473:511–525.
- Deleuze C, Huguenard JR (2006) Distinct electrical and chemical connectivity maps in the thalamic reticular nucleus: potential roles in synchronization and sensation. *J Neurosci* 26:8633–8645.
- Destexhe A (1998) Spike-and-wave oscillations based on the properties of GABAB receptors. *J Neurosci* 18:9099–9111.
- Devor A, Yarom Y (2002) Electrotonic coupling in the inferior olivary nucleus revealed by simultaneous double patch recordings. *J Neurophysiol* 87:3048–3058.
- DeVries SH, Qi X, Smith R, Makous W, Sterling P (2002) Electrical coupling between mammalian cones. *Curr Biol* 12:1900–1907.
- Domich L, Oakson G, Steriade M (1986) Thalamic burst patterns in the naturally sleeping cat: a comparison between cortically projecting and reticularis neurones. *J Physiol* 379:429–449.
- Dugué GP, Brunel N, Hakim V, Schwartz E, Chat M, Lévesque M, Courtemanche R, Léna C, Dieudonné S (2009) Electrical coupling mediates tunable low-frequency oscillations and resonance in the cerebellar Golgi cell network. *Neuron* 61:126–139.
- Dunn FA, Doan T, Sampath AP, Rieke F (2006) Controlling the gain of rod-mediated signals in the mammalian retina. *J Neurosci* 26:3959–3970.
- Feig S, Harting JK (1998) Corticocortical communication via the thalamus: ultrastructural studies of corticothalamic projections from area 17 to the lateral posterior nucleus of the cat and inferior pulvinar nucleus of the owl monkey. *J Comp Neurol* 395:281–295.
- Fernandez FR, Via G, Canavier CC, White JA (2022) Kinetics and connectivity properties of parvalbumin- and somatostatin-positive inhibition in layer 2/3 medial entorhinal cortex. *Eneuro* 9:1–14.
- Fernandez LM, Vantomme G, Osorio-Forero A, Cardis R, Béard E, Lüthi A (2018) Thalamic reticular control of local sleep in mouse sensory cortex. *Elife* 7:e39111.
- Fitzpatrick D, Usrey WM, Schofield BR, Einstein G (1994) The sublamina organization of corticogeniculate neurons in layer 6 of macaque striate cortex. *Vis Neurosci* 11:307–315.
- Fonnum F, Storm-Mathisen J, Divac I (1981) Biochemical evidence for glutamate as neurotransmitter in corticostriatal and corticothalamic fibres in rat brain. *Neuroscience* 6:863–873.
- Fortier PA (2010) Detecting and estimating rectification of gap junction conductance based on simulations of dual-cell recordings from a pair and a network of coupled cells. *J Theor Biol* 265:104–114.
- Fosse VM, Kolstad J, Fonnum F (1986) A bioluminescence method for the measurement of l-glutamate: applications to the study of changes in the release of l-glutamate from lateral geniculate nucleus and superior colliculus after visual cortex ablation in rats. *J Neurochem* 47:340–349.
- Frasconi C, Bentivoglio M, Spreafico R, Sánchez MP, Puelles L, Fairen A (1991) Postnatal development of calbindin and parvalbumin immunoreactivity in the thalamus of the rat. *Dev Brain Res* 58:243–249.
- Fricke B, Heckman E, Cunningham PC, Wang H, Haas JS (2021) Activity-dependent long-term potentiation of electrical synapses in the mammalian thalamus. *J Neurophysiol* 125:476–488.
- Fuentealba P, Crochet S, Timofeev I, Bazhenov M, Sejnowski TJ, Steriade M (2004) Experimental evidence and modeling studies support a synchronizing role for electrical coupling in the cat thalamic reticular neurons in vivo. *Eur J Neurosci* 20:111–119.
- Galarreta M, Hestrin S (1999) A network of fast-spiking cells in the neocortex connected by electrical synapses. *Nature* 402:72–75.
- Galarreta M, Erdélyi F, Szabó G, Hestrin S (2004) Electrical coupling among irregular-spiking GABAergic interneurons expressing cannabinoid receptors. *J Neurosci* 24:9770–9778.
- Gibson JR, Beierlein M, Connors BW (1999) Two networks of electrically coupled inhibitory neurons in neocortex. *Nature* 402:75–79.

- Haas JS, Landisman CE (2011) State-dependent modulation of gap junction signaling by the persistent sodium current. *Front Cell Neurosci* 5:31.
- Haas JS, Zavala B, Landisman CE (2011) Activity-dependent long-term depression of electrical synapses. *Science* 334:389–393.
- Halassa MM, Siegle JH, Ritt JT, Ting JT, Feng G, Moore CI (2011) Selective optical drive of thalamic reticular nucleus generates thalamic bursts and cortical spindles. *Nat Neurosci* 14:1118–1120.
- Halassa MM, Chen Z, Wimmer RD, Brunetti PM, Zhao S, Zikopoulos B, Wang F, Brown EN, Wilson MA (2014) State-dependent architecture of thalamic reticular subnetworks. *Cell* 158:808–821.
- Hatch RJ, Mendis GDC, Kaila K, Reid CA, Petrou S (2017) Gap junctions link regular-spiking and fast-spiking interneurons in layer 5 somatosensory cortex. *Front Cell Neurosci* 11:204.
- Hoseini MS, Higashikubo B, Cho FS, Chang AH, Clemente-Perez A, Lew I, Ciesielska A, Stryker MP, Paz JT (2021) Gamma rhythms and visual information in mouse V1 specifically modulated by somatostatin+ neurons in reticular thalamus. *Elife* 10:e61437.
- Hou G, Smith AG, Zhang ZW (2016) Lack of intrinsic GABAergic connections in the thalamic reticular nucleus of the mouse. *J Neurosci* 36:7246–7252.
- Hu H, Cavendish JZ, Agmon A (2013) Not all that glitters is gold: off-target recombination in the somatostatin-IRES-Cre mouse line labels a subset of fast-spiking interneurons. *Front Neural Circuits* 7:195.
- Inoue M, Duysens J, Vossen JM, Coenen AM (1993) Thalamic multiple-unit activity underlying spike-wave discharges in anesthetized rats. *Brain Res* 612:35–40.
- Jones E (1975) Some aspects of the organization of the thalamic reticular complex. *J Comp Neurol* 162:285–308.
- Jones E, Hendry S (1989) Differential calcium binding protein immunoreactivity distinguishes classes of relay neurons in monkey thalamic nuclei. *Eur J Neurosci* 1:222–246.
- Kocaturk S, Guven EB, Shah F, Tepper JM, Assous M (2022) Cholinergic control of striatal GABAergic microcircuits. *Cell Rep* 41:111531.
- Kohmann D, Lüttjohann A, Seidenbecher T, Coulon P, Pape HC (2016) Short-term depression of gap junctional coupling in reticular thalamic neurons of absence epileptic rats. *J Physiol* 594:5695–5710.
- Lam Y-W, Sherman SM (2007) Different topography of the reticulothalamic inputs to first- and higher-order somatosensory thalamic relays revealed using photostimulation. *J Neurophysiol* 98:2903–2909.
- Landisman CE, Connors BW (2005) Long-term modulation of electrical synapses in the mammalian thalamus. *Science* 310:1809–1813.
- Landisman CE, Long MA, Beierlein M, Deans MR, Paul DL, Connors BW (2002) Electrical synapses in the thalamic reticular nucleus. *J Neurosci* 22:1002–1009.
- Lee S-C, Patrick SL, Richardson KA, Connors BW (2014) Two functionally distinct networks of gap junction-coupled inhibitory neurons in the thalamic reticular nucleus. *J Neurosci* 34:13170–13182.
- Lewis LD, Voigts J, Flores FJ, Schmitt LI, Wilson MA, Halassa MM, Brown EN (2015) Thalamic reticular nucleus induces fast and local modulation of arousal state. *Elife* 4:e08760.
- Li X, Itani O, Bucher DM, Rotstein HG, Nadim F (2023) Distinct mechanisms underlie electrical coupling resonance and its interaction with membrane potential resonance. *Front Syst Biol* 3:1122433.
- Li Y, Lopez-Huerta VG, Adiconis X, Levandowski K, Choi S, Simmons SK, Arias-Garcia MA, Guo B, Yao AY, Blosser TR (2020) Distinct subnetworks of the thalamic reticular nucleus. *Nature* 583:819–824.
- Liu XB, Jones EG (1999) Predominance of corticothalamic synaptic inputs to thalamic reticular nucleus neurons in the rat. *J Comp Neurol* 414:67–79.
- Lizier C, Spreafico R, Battaglia G (1997) Calretinin in the thalamic reticular nucleus of the rat: distribution and relationship with ipsilateral and contralateral efferents. *J Comp Neurol* 377:217–233.
- Long MA, Landisman CE, Connors BW (2004) Small clusters of electrically coupled neurons generate synchronous rhythms in the thalamic reticular nucleus. *J Neurosci* 24:341–349.
- Marlinski V, Beloozerova IN (2014) Burst firing of neurons in the thalamic reticular nucleus during locomotion. *J Neurophysiol* 112:181–192.
- Martinez-Garcia RI, Voelcker B, Zaltsman JB, Patrick SL, Stevens TR, Connors BW, Cruikshank SJ (2020) Two dynamically distinct circuits driving inhibition in sensory thalamus. *bioRxiv*.
- McAlonan K, Cavanaugh J, Wurtz RH (2006) Attentional modulation of thalamic reticular neurons. *J Neurosci* 26:4444–4450.
- McCafferty C, David F, Venzi M, Lőrincz ML, Delicata F, Atherton Z, Recchia G, Orban G, Lambert RC, Di Giovanni G (2018) Cortical drive and thalamic feed-forward inhibition control thalamic output synchrony during absence seizures. *Nat Neurosci* 21:744–756.
- Medvedev GS (2009) Electrical coupling promotes fidelity of responses in the networks of model neurons. *Neural Comput* 21:3057–3078.
- Mendoza AJ, Haas JS (2022) Intrinsic sources and functional impacts of asymmetry at electrical synapses. *Eneuro* 9.
- Minderhoud J (1971) An anatomical study of the efferent connections of the thalamic reticular nucleus. *Exp Brain Res* 12:435–446.
- Mitrofanis J (1992a) Patterns of antigenic expression in the thalamic reticular nucleus of developing rats. *J Comp Neurol* 320:161–181.
- Mitrofanis J (1992b) Calbindin immunoreactivity in a subset of cat thalamic reticular neurons. *J Neurocytol* 21:495–505.
- Nakajima M, Schmitt LI, Halassa MM (2019) Prefrontal cortex regulates sensory filtering through a basal ganglia-to-thalamus pathway. *Neuron* 103:445–458.e10.
- Ni K-M, Hou X-J, Yang C-H, Dong P, Li Y, Zhang Y, Jiang P, Berg DK, Duan S, Li X-M (2016) Selectively driving cholinergic fibers optically in the thalamic reticular nucleus promotes sleep. *Elife* 5:e10382.
- Oh SW, Harris JA, Ng L, Winslow B, Cain N, Mihalas S, Wang Q, Lau C, Kuan L, Henry AM (2014) A mesoscale connectome of the mouse brain. *Nature* 508:207–214.
- Ohara P (1988) Synaptic organization of the thalamic reticular nucleus. *J Electron Microscop Tech* 10:283–292.
- Ohara PT, Lieberman A (1985) The thalamic reticular nucleus of the adult rat: experimental anatomical studies. *J Neurocytol* 14:365–411.
- Onn SP, Grace AA (1999) Alterations in electrophysiological activity and dye coupling of striatal spiny and aspiny neurons in dopamine-denervated rat striatum recorded in vivo. *Synapse* 33:1–15.
- Parker PR, Cruikshank SJ, Connors BW (2009) Stability of electrical coupling despite massive developmental changes of intrinsic neuronal physiology. *J Neurosci* 29:9761–9770.
- Pham T, Haas JS (2018) Electrical synapses between inhibitory neurons shape the responses of principal neurons to transient inputs in the thalamus: a modeling study. *Sci Rep* 8:7763.
- Pinault D (2004) The thalamic reticular nucleus: structure, function and concept. *Brain Res Brain Res Rev* 46:1–31.
- Pinault D, Deschenes M (1998) Projection and innervation patterns of individual thalamic reticular axons in the thalamus of the adult rat: a three-dimensional, graphic, and morphometric analysis. *J Comp Neurol* 391:180–203.
- Schoppa NE, Westbrook GL (2002) AMPA autoreceptors drive correlated spiking in olfactory bulb glomeruli. *Nat Neurosci* 5:1194–1202.
- Seto-Ohshima A, Emson P, Berchtold M, Heizmann C (1989) Localization of parvalbumin mRNA in rat brain by in situ hybridization histochemistry. *Exp Brain Res* 75:653–658.
- Sevetson J, Haas JS (2015) Asymmetry and modulation of spike timing in electrically coupled neurons. *J Neurophysiol* 113:1743–1751.
- Sevetson J, Fittro S, Heckman E, Haas JS (2017) A calcium-dependent pathway underlies activity-dependent plasticity of electrical synapses in the thalamic reticular nucleus. *J Physiol* 595:4417–4430.
- Sherman SM (2016) Thalamus plays a central role in ongoing cortical functioning. *Nat Neurosci* 19:533–541.
- Sigulinsky CL, Anderson JR, Kerzner E, Rapp CN, Pfeiffer RL, Rodman TM, Emrich DP, Rapp KD, Nelson NT, Lauritzen JS (2020) Network architecture of gap junctional coupling among parallel processing channels in the mammalian retina. *J Neurosci* 40:4483–4511.

- Simon A, Oláh S, Molnár G, Szabadics J, Tamás G (2005) Gap-junctional coupling between neurogliaform cells and various interneuron types in the neocortex. *J Neurosci* 25:6278–6285.
- Steriade M (2005) Sleep, epilepsy and thalamic reticular inhibitory neurons. *Trends Neurosci* 28:317–324.
- Steriade M, Llinás RR (1988) The functional states of the thalamus and the associated neuronal interplay. *Physiol Rev* 68:649–742.
- Tamás G, Buhl EH, Lőrincz A, Somogyi P (2000) Proximally targeted GABAergic synapses and gap junctions synchronize cortical interneurons. *Nat Neurosci* 3:366–371.
- Thankachan S, Katsuki F, McKenna JT, Yang C, Shukla C, Deisseroth K, Uygun DS, Strecker RE, Brown RE, McNally JM (2019) Thalamic reticular nucleus parvalbumin neurons regulate sleep spindles and electrophysiological aspects of schizophrenia in mice. *Sci Rep* 9:3607.
- Vantomme G, Osorio-Forero A, Lüthi A, Fernandez LM (2019) Regulation of local sleep by the thalamic reticular nucleus. *Front Neurosci* 13:576.
- Vaughn MJ, Haas JS (2022) On the diverse functions of electrical synapses. *Front Cell Neurosci* 16:910015.
- Venance L, Rozov A, Blatow M, Burnashev N, Feldmeyer D, Monyer H (2000) Connexin expression in electrically coupled postnatal rat brain neurons. *Proc Natl Acad Sci U S A* 97:10260–10265.
- Wang Z, Neely R, Landisman CE (2015) Activation of group I and group II metabotropic glutamate receptors causes LTD and LTP of electrical synapses in the rat thalamic reticular nucleus. *J Neurosci* 35:7616–7625.
- Warren RA, Jones EG (1997) Maturation of neuronal form and function in a mouse thalamo-cortical circuit. *J Neurosci* 17:277–295.
- Whilden CM, Chevée M, An SY, Brown SP (2021) The synaptic inputs and thalamic projections of two classes of layer 6 corticothalamic neurons in primary somatosensory cortex of the mouse. *J Comp Neurol* 529:3751–3771.
- Wimmer RD, Schmitt LI, Davidson TJ, Nakajima M, Deisseroth K, Halassa MM (2015) Thalamic control of sensory selection in divided attention. *Nature* 526:705–709.
- Zhang L, Jones EG (2004) Corticothalamic inhibition in the thalamic reticular nucleus. *J Neurophysiol* 91:759–766.
- Zikopoulos B, Barbas H (2012) Pathways for emotions and attention converge on the thalamic reticular nucleus in primates. *J Neurosci* 32:5338–5350.
- Zolnik TA, Connors BW (2016) Electrical synapses and the development of inhibitory circuits in the thalamus. *J Physiol* 594:2579–2592.
- Zsiros V, Maccaferri G (2005) Electrical coupling between interneurons with different excitable properties in the stratum lacunosum-moleculare of the juvenile CA1 rat hippocampus. *J Neurosci* 25:8686–8695.